Long-term carbon storage in shelf sea sediments reduced by intensive bottom trawling

Wenyan Zhang [1] ✉, Lucas Porz [1], Rümeysa Yilmaz[1], Klaus Wallmann [2], Timo Spiegel [2], Andreas Neumann[3], Moritz Holtappels [4,5], Sabine Kasten[4,5,6], Jannis Kuhlmann [7], Nadja Ziebarth[7], Bettina Taylor[7], Ha Thi Minh Ho-Hagemann [1], Frank-Detlef Bockelmann[3], Ute Daewel[1], Lea Bernhardt [8,9] & Corinna Schrum [1,10]

Bottom trawling represents the most widespread anthropogenic physical disturbance to seafloor sediments on continental shelves. While trawling-induced changes to benthic ecology have been widely recognized, the impacts on long-term organic carbon storage in marine sediments remains uncertain. Here we combined datasets of sediment and bottom trawling for a heavily trawled region, the North Sea, to explore their potential mutual dependency. A pattern emerges when comparing the surface sediment organic carbon-to-mud ratio with the trawling intensity represented by the multi-year averaged swept area ratio. The organic carbon-to-mud ratio exhibits a systematic response to trawling where the swept area ratio is larger than 1 yr^{-1}. Three-dimensional physical–biogeochemical simulation results suggest that the observed pattern is attributed to the correlated dynamics of mud and organic carbon during transport and redeposition in response to trawling. Both gain and loss of sedimentary organic carbon may occur in weakly trawled areas, whereas a net reduction of sedimentary organic carbon is found in intensely trawled grounds. Cessation of trawling allows restoration of sedimentary carbon stock and benthic biomass, but their recovery occurs at different timescales. Our results point out a need for management of intensely trawled grounds to enhance the CO_2 sequestration capacity in shelf seas.

Bottom trawling, as a widely used fishing technique, resuspends more than 20 Gt of sediment annually on global continental shelves[1], representing the most widespread anthropogenic physical disturbance to surface sediments and benthic habitats[2–6]. Although bottom trawling has been performed in coastal regions for over a century, quantifying its impact on benthic biota and biogeochemical cycling has become a focal point of research only in recent decades[2,3,7,8].

Bottom trawling restructures and resuspends the upper layers of seafloor sediments and thereby alters benthic faunal communities[7,9],

early diagenesis and element fluxes across the sediment–water interface[10]. A recent study[3] highlighted the impact of bottom trawling on organic carbon (OC) storage in surface seabed and suggested that trawling causes remineralization of 0.16–0.4 Gt sedimentary OC globally every year, equivalent to 0.58–1.47 GtCO_2 efflux from the sediment–water interface. This estimate was subsequently questioned by several authors[4,5], who emphasized that there is no consensus in the existing literature on whether or to what extent trawling would lead to reduced OC storage.
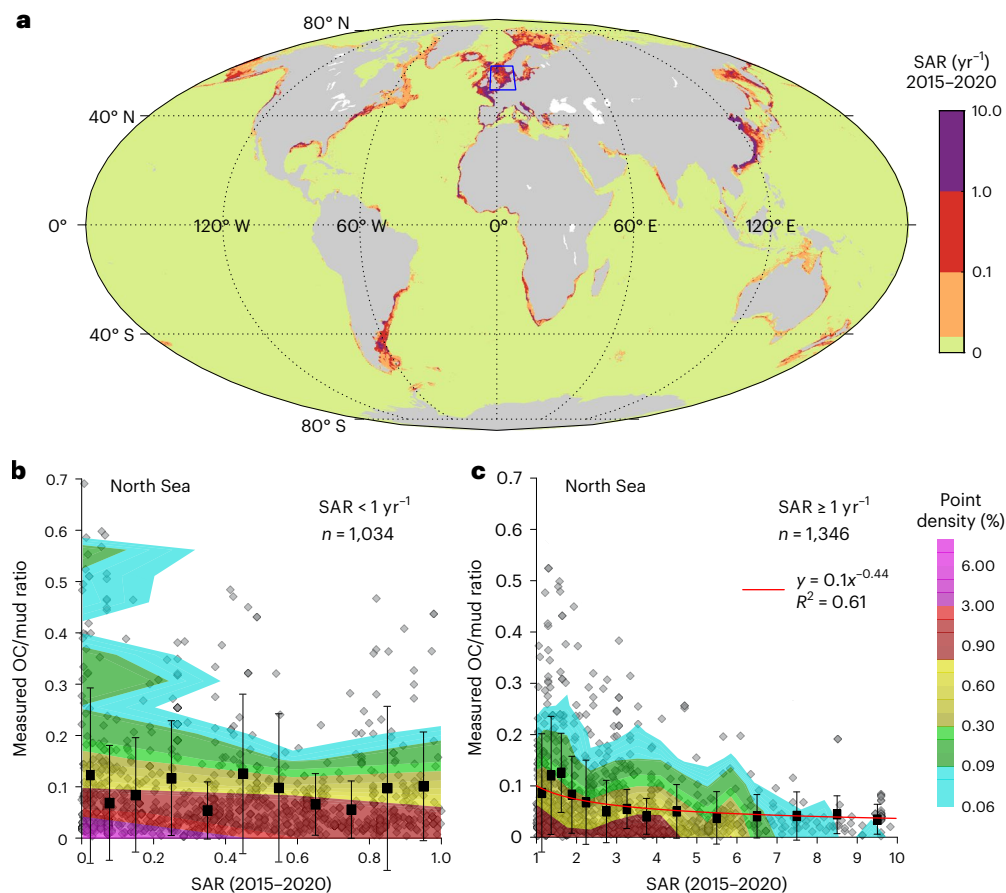
Fig. 1 | Relationship between bottom trawling and OC/mud in the North Sea surface sediments. a, Qualitative estimate of global distribution of SAR (yr⁻¹) calculated on the basis of fishing effort data in ref. 23, averaged for 2015–2020 and assuming all trawlers in global shelf seas are bottom trawlers. **b,** Distribution of point data of OC/mud in relation to SAR in weakly or untrawled areas (SAR < 1 yr⁻¹, *n* = 1,034) in the North Sea. **c,** Similar to **b** but for intensely trawled

areas (SAR ≥ 1 yr⁻¹, *n* = 1,346). The aggregates for calculation of mean ± standard deviation (indicated by dots and error bars) are determined in such a way that the number of points in each aggregated interval is of the same order of magnitude (Supplementary Fig. 3), namely, 75–150 points per interval in **b** and 35–150 points per interval in **c**, to avoid biased statistics.

To understand the impact of bottom trawling on OC storage in seabed, it is crucial to disentangle the linkages among the involved processes. In shelf seas, slow-sinking particulate organic matter (POM) is remineralized mostly in the water column, and POM that reaches the seafloor is generally featured by large size (>50 μm) with high sinking velocity[11], attributed mainly to flocculation with (or sorption on) fine-grained sediments (silts and clay, collectively termed as mud)[12]. Therefore, POM in the benthic zone has similar physical properties with mud regarding transport and settling. However, resuspended POM can be remineralized at an enhanced rate in oxic bottom water compared with anoxic sediments[13,14]. Because of an influence of OC remineralization by mud, the OC-to-mineral surface area ratio has been used for assessing the potential of OC preservation in sediments[15,16] and identification of anthropogenic impact[17]. By analogy with the OC-to-mineral surface area ratio, the OC-to-mud ratio (OC/mud), which is easier to measure for a large number of sediment samples, is used as an alternative indicator in our analysis. We hypothesize that trawling would lead to a difference of OC/mud between untrawled and trawled seabed.

During recent years, increasing effort has been made to map seabed carbon content at regional[18,19] and global scales[20,21]. In addition, the combination of satellite-based monitoring systems and logbook data has enabled estimates of bottom-trawling intensity with high spatial and temporal resolution[22–24]. Combining the information of sediment property and trawling intensity allows us to explore their potential

relationship. In this Article, we compile and analyse relevant data for a heavily trawled region, the North Sea (Fig. 1), to identify the linkage between OC storage and trawling. We then apply three-dimensional physical–biogeochemical modelling to disentangle the involved processes and discuss their implication at global scale.

Linkage between trawling and sediment OC/mud ratio

The multi-year (2015–2020) averaged swept area ratio (SAR, yr⁻¹), the ratio between the cumulative area touched by bottom-trawling gears averaged over the period of 2015–2020 and the area of the respective grid cell (0.05° × 0.05°), is used as an indicator for trawling intensity. The North Sea has been heavily trawled for many decades[25] with SAR > 1 yr⁻¹ in over 30% of its area (Supplementary Fig. 1). SAR exhibits a weak correlation with surface sediment OC content (*r* = 0.12, *P* < 0.001) and mud content (*r* = 0.23, *P* < 0.001) (Supplementary Fig. 2). However, OC content is strongly correlated with mud content (*r* = 0.66, *P* < 0.001), indicating an increasing storage of OC along with an increasing mud content.

Despite the independence between trawling intensity and sediment OC content, a pattern emerges when comparing the SAR and OC/mud (Fig. 1b,c). The OC/mud is relatively scattered where SAR < 1 yr⁻¹ and exhibits no clear trend in the mean value and standard deviation among the different intervals. However, OC/mud is confined to a narrower and lower range where SAR > 1 yr⁻¹. The impact of
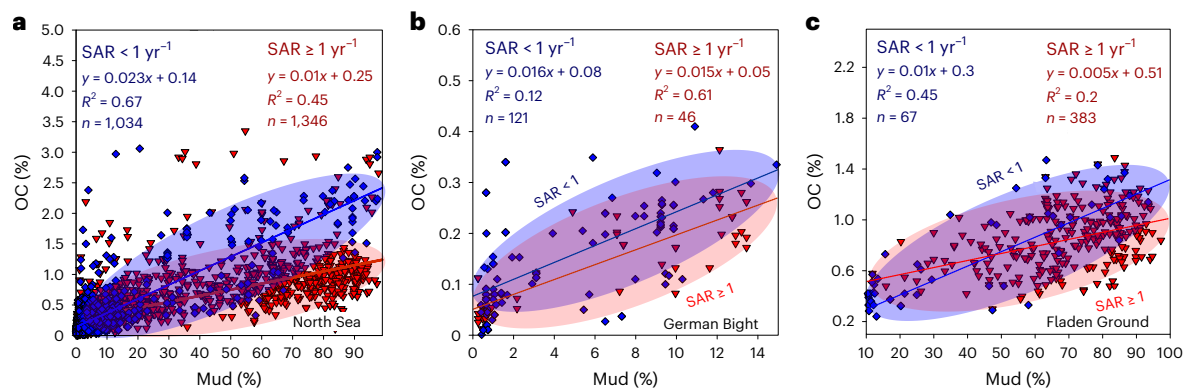
Fig. 2 | Impact of bottom-trawling intensity on the OC–mud relationship in the North Sea sediments. a, Data points and relationship are distinguished by weak or zero trawling intensity (SAR < 1 yr⁻¹, n = 1,034) and enhanced trawling intensity (SAR ≥ 1 yr⁻¹, n = 1,346) for the entire North Sea. **b,c**, Data from two densely sampled local areas (location in Supplementary Fig. 4) representing sandy (German Bight, n = 167) (**b**) and muddy (Fladen Ground, n = 450) (**c**) seabed. The ellipses contain at least 80% of data points for the two groups bounded by SAR = 1 yr⁻¹. Linear trendlines are shown with corresponding functions and R squared.

trawling on the relationship between mud and OC is notable by comparing weakly or untrawled sites with intensely trawled sites (Fig. 2). A negative impact of SAR on OC is further confirmed by our multivariate analysis (Extended Data Table 1), which shows that an increase of SAR by 1 yr⁻¹ corresponds to an average decrease in OC content by 0.016 ± 0.005 percentage points. This relationship is particularly significant for SAR ≥ 1 yr⁻¹, but not for SAR < 1 yr⁻¹ (Extended Data Table 2).

Process-based understanding of trawling impact

The OC storage in seabed is controlled by an interplay between pelagic and benthic processes[26–29] (Fig. 3a). Pelagic biota, mainly plankton, provides an important source of OC in shelf sea sediments[26]. Freshly produced OC may undergo a series of resuspension–transport–deposition cycles before being buried in sediments and/or utilized by benthic fauna[27] and microbial communities[30]. Remineralization of OC occurs during both transport and burial processes, depending on a variety of environmental parameters, with oxygen exposure as an essential controlling factor[13,14].

The blurred picture of bottom-trawling effects on OC storage in sediments originates from several counteracting mechanisms (Fig. 3b). On the one hand, trawling-induced resuspension and physical mixing of sediments may enhance OC remineralization by increasing oxygen exposure time and limit OC storage by inhibiting deposition of mud[13,14,31–33]. On the other hand, intensified lateral transport towards offshore depocentres and increase in primary production caused by trawling-resuspended nutrients may offset the OC loss to varying extents[34–36]. The complexity is further increased by benthic fauna, which not only contribute to OC but also mediate OC fluxes across the sediment–water interface[26–29]. The recognized effect of trawling on macrobenthos is a depletion of biomass and change of the community from sessile to mobile and opportunistic species[37–40]. However, for quantitative assessments of how trawling-induced impacts on benthic fauna would affect OC storage, the current evidence base is incomplete[4–6,28,41].

To quantify the individual and combined impacts of the various processes associated with trawling, we applied a three-dimensional physical–biogeochemical model to the North Sea (Methods). In total, 19 sensitivity experiments were investigated to assess the uncertainty caused by assumptions or empirical parameterizations in the model regarding trawling impacts (Supplementary Table 1). We calculated the mean (ensemble average) and standard deviation of simulation results from the 18 experiments in which trawling impacts are considered to various extents and compared with the reference simulation excluding trawling impact. Our results indicate that although trawling modifies

the total annual benthic remineralization of OC to only a small extent, its impact significantly affects the net OC flux across the sediment–water interface (Fig. 3c).

In the scenario without trawling impact (No trawling), the annual aggregated deposition of fresh OC is relatively stable at 119 ± 10 Mg km⁻² yr⁻¹. However, most of the deposition is transient and undergoes natural resuspension–transport–deposition cycles until being remineralized (104 ± 8 Mg km⁻² yr⁻¹). Benthic fauna plays an important role in both remineralization and preservation of OC. Bioturbation-induced remineralization contributes to 25–30% of total benthic remineralization, at 28 ± 5 Mg km⁻² yr⁻¹. Macrobenthos respiration additionally consumes OC at 14 ± 2.5 Mg km⁻² yr⁻¹. However, bioturbation-induced downward transport of OC (57 ± 9 Mg km⁻² yr⁻¹) into deeper sediment horizons, where oxygen is reduced or absent, facilitates the long-term OC storage. Because of these natural processes, OC accumulates in the seabed sediments of the 'untrawled' North Sea at 1.5 ± 1.1 Mg km⁻² yr⁻¹.

In the trawling scenarios, trawling annually resuspends 54 ± 18 MgC km⁻² yr⁻¹ (including carbon from newly added detritus and existing material), which subsequently enters the resuspension–transport–deposition cycles. OC remineralization resulting from trawling-induced resuspension and physical mixing amounts to 11 ± 4 Mg km⁻² yr⁻¹, contributing to ~10% of total benthic remineralization (110 ± 10 Mg km⁻² yr⁻¹). Owing to trawling-induced mortality, remineralization caused by bioturbation and fauna respiration are reduced to 22 ± 5 and 11 ± 3 Mg km⁻² year⁻¹, respectively, which partly offsets the loss. However, bioturbation-induced downward transport of OC is reduced by ~25% to 43 ± 8 Mg km⁻² yr⁻¹. This reduction is only slightly compensated by trawling-induced physical mixing at 2.5 ± 1 Mg km⁻² yr⁻¹. These terms jointly lead to a change in the net accumulation rate of OC to 0.4 ± 1 Mg km⁻² yr⁻¹. In years characterized by reduced OC deposition, the net OC flux is negative, meaning that the surface seabed turns into a source of carbon in the water column due to a net loss of OC caused by trawling (Supplementary Fig. 5). In the 18 sensitivity experiments, the largest variation occurs among the simulations using different trawling-induced macrobenthos mortality rates, suggesting an important control of benthic fauna in OC storage and turnover (Supplementary Fig. 6).

The trawling-induced reduction of macrobenthos biomass in our simulations is consistent with the estimates in ref. 42, who combined trawling pressure, gear characteristics, habitat characteristics and sensitivity of benthic community to assess impact of bottom trawling. Their results suggest a 13% trawling-induced reduction of total biomass in the North Sea, with the highest reduction (26%) in mud seabed and
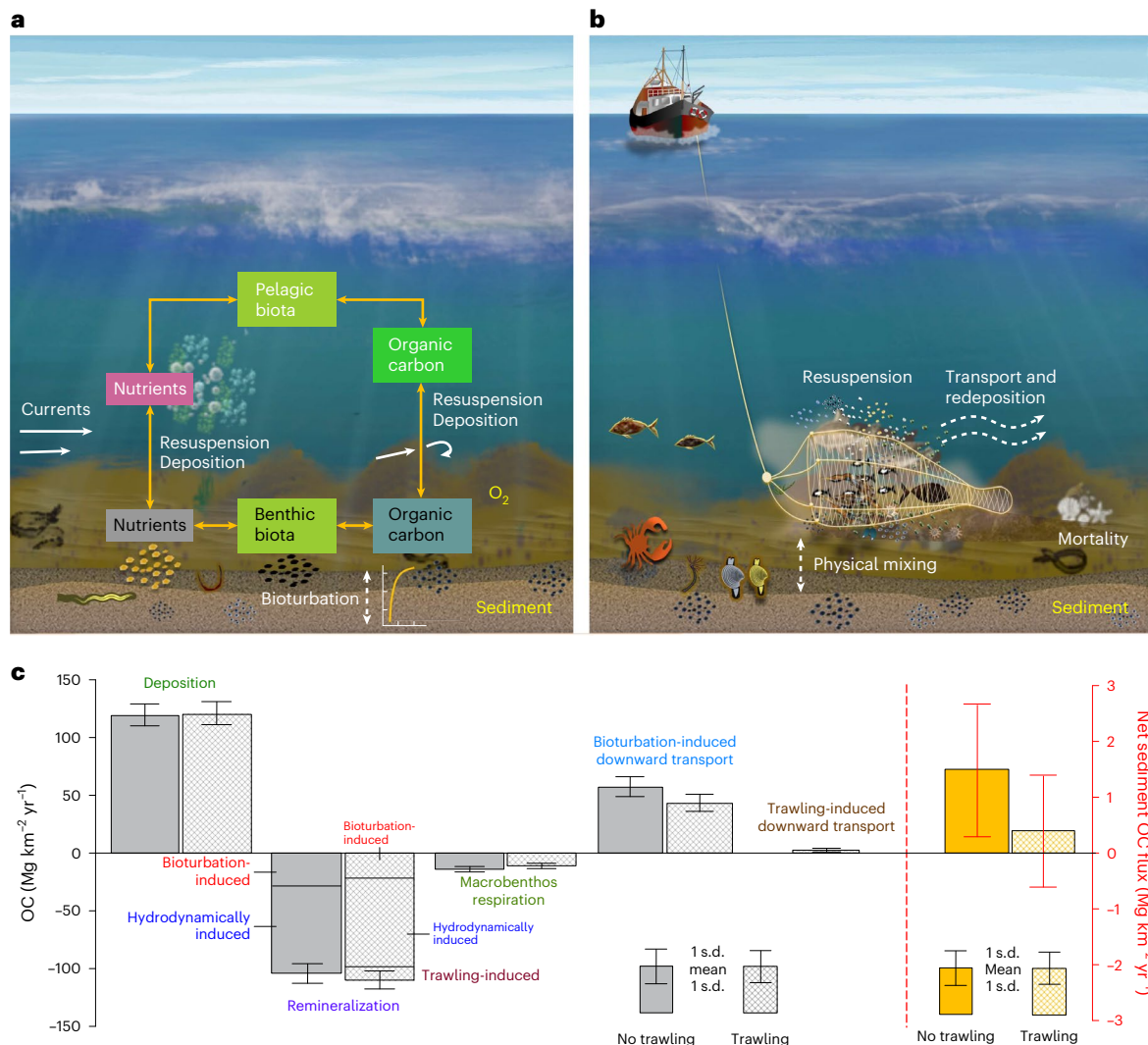
Fig. 3 | Process-based understanding of OC cycling and storage in surface sediments. a, Benthic–pelagic coupling in a natural system. **b**, Processes involved in bottom trawling. **c**, Model-estimated source and sink terms of OC in surface sediments in the No-trawling (n = 67 annual values for 1950–2016) and trawling (n = 67 ensemble-averaged values for 1950–2016) scenarios of the North Sea. Note that only freshly produced OC is counted in all terms displayed in **c**. Bioturbation- and trawling-induced downward transports refer to the fluxes across the uppermost 1 cm within the sediment. Positive values on the y axis on the right side of **c** indicate influx of OC from water to sediments, and negative values refer to OC outflux from sediments to water.

the lowest reduction (9%) in coarse sediments. Similar patterns are also seen in our ensemble-averaged results (Fig. 4c), with biomass reductions of up to 30% in frequently trawled (SAR > 5 yr^{-1}) mud depocentres and up to 15% in sandy seabed. Meanwhile, some untrawled and weakly trawled areas feature a slight increase of biomass (<5%) due to deposition of resuspended OC from adjacent trawled areas.

Labile and semi-labile OC in surface sediments are particularly susceptible to trawling impact[10]. Like the spatial patterns in the change of macrobenthos biomass, frequently trawled muddy areas show the largest reduction of OC (10–25%) compared with the No-trawling scenario, while frequently trawled sandy areas feature a 5–10% OC reduction (Fig. 4d). Meanwhile, untrawled and weakly trawled areas are characterized by a slight OC increase (≤10%) due mainly to deposition of resuspended OC from adjacent trawled areas. However, this increase only partly offsets the net decrease.

In the No-trawling scenario, OC/mud is generally higher when compared with the field data (Fig. 5a), while the simulations including trawling yield results closer to the field data (Fig. 5b). A similar pattern in the distribution of OC/mud in relation to SAR is shown in the simulation result after 50 years of trawling (Supplementary Fig. 7). The decline of OC/mud is attributed mainly to reduction of OC because

of a larger relative change of OC content than mud content caused by trawling, particularly in a major part of intensively trawled areas where both mud and OC content are reduced (Supplementary Fig. 8). According to the ensemble average of all trawling scenarios, the relative change in OC/mud between the simulations with and without trawling after 10 years shows that areas with SAR < 1 yr^{-1} feature both carbon gain (48%) and carbon loss (52%), while areas with SAR > 1 yr^{-1} are dominated by OC loss that increases with SAR (Fig. 5c). The relative change of the means aggregated in intervals of ΔSAR = 1 yr^{-1} follows a power function ($y = 0.96x^{-0.1}$, $R^2 = 0.79$). After 50 years of persistent trawling impact, the relative change of OC/mud shows a similar pattern with the result after 10 years (Fig. 5d), but with an increasing trend towards lower OC/mud along with increasing SAR ($y = 0.96x^{-0.13}$, $R^2 = 0.81$). Over the entire North Sea, 32% and 68% of areas where SAR < 1 yr^{-1} are characterized by OC gain and loss, respectively. By contrast, more than 90% of areas where SAR > 1 yr^{-1} experience a net OC loss (Fig. 5d).

To identify the trawling impact on different habitats of the North Sea, we divided the seabed into two types: sand (mud content < 5%) and muddy sediments. Field data indicate that OC/mud in sand is relatively scattered, with mean value between 0.1 and 0.2, while in muddy sediments it is mostly below 0.1 (Fig. 6a,b). The difference is significant
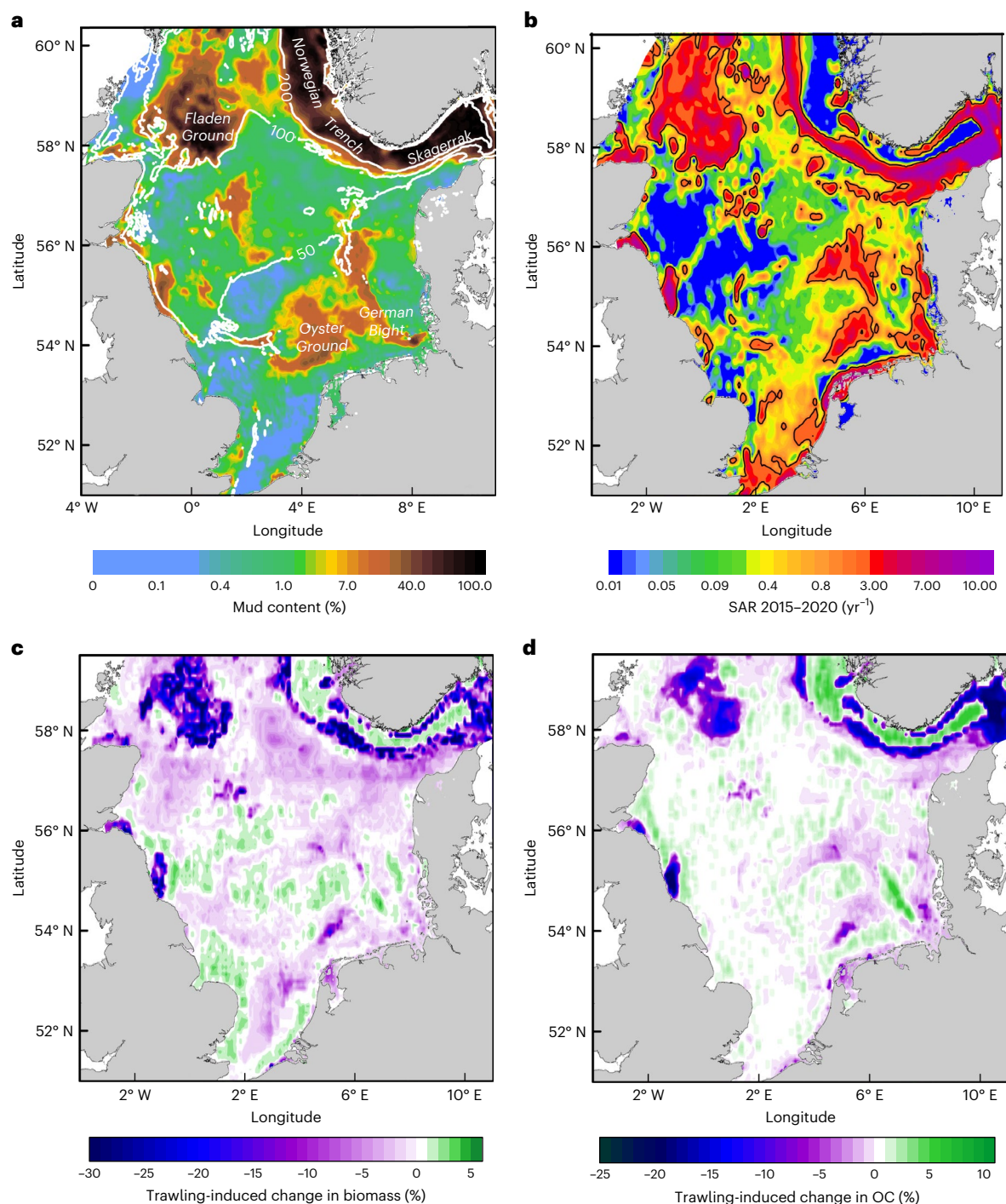
Fig. 4 | Spatial distribution of sediment property, bottom-trawling intensity and simulated change of benthic faunal biomass and OC content in the North Sea surface sediments. a, Mean mud content (%) in the upper 10 cm sediment, with marked large-scale mud depocentres. **b**, Synthesized annual SAR averaged over the period of 2015–2020. The contour line of SAR = 1 yr^{-1} is indicated. **c,d**, Ensemble-averaged trawling-induced relative changes in macrobenthos biomass (**c**) and sedimentary OC (**d**) after 50 years. Positive and negative values refer to increase and reduction in percentage, respectively.

(Extended Data Table 3). The scattered distribution of OC/mud in sand is partly due to the natural dynamics of mud and OC accumulation in sand[30] and partly affected by trawling, since there exists a decreasing trend with increasing SAR. This is confirmed by the simulation showing that carbon gain and loss both occur where SAR is low, but carbon loss gradually dominates with increasing SAR (Fig. 6c). Carbon content in muddy sediments exhibits a similar response pattern to trawling, but with an enhanced decreasing trend with increasing SAR compared with sand (Fig. 6a,b), suggesting a higher vulnerability of carbon to trawling

impact in muddy habitats. This is confirmed by our simulations, albeit to a smaller extent (Fig. 6c,d).

Implications for global bottom-trawling impact

The spatio-temporal complexity in the response of shelf sea sediment carbon storage to bottom trawling is reflected in current debates[3–6]. Our study addresses this complexity by analysing the change of OC/mud in response to trawling intensity and by modelling natural and trawling-associated processes in OC turnover. The implications
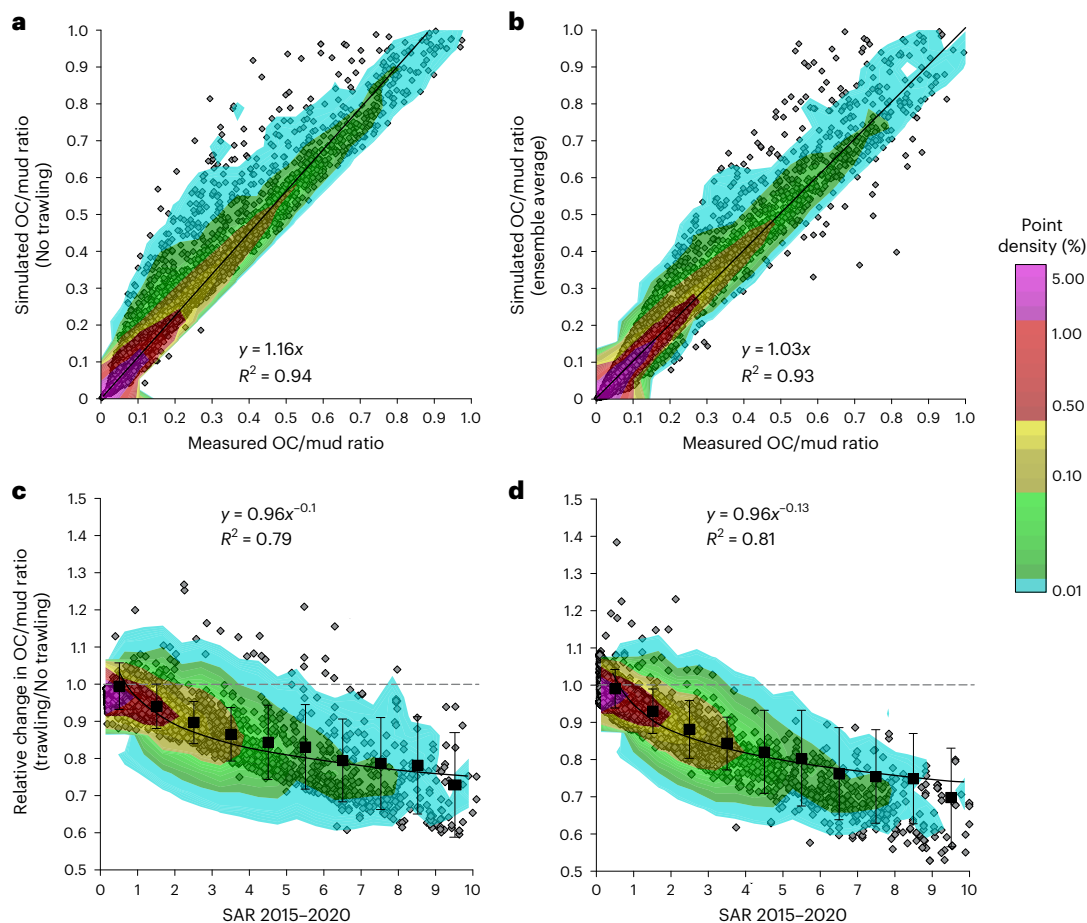
Fig. 5 | Difference of carbon content in mud between measured field data and simulations with and without trawling impacts in the North Sea. **a**, Measured OC/mud and simulation without trawling impact for 50 years (No trawling, $n = 2,380$). **b**, Similar to **a** but for simulation with trawling impact.

c, Relative change of OC/mud between simulations with and without trawling for 10 years. The means ± standard deviations are indicated by dots and error bars. **d**, Similar to **c** but for 50 years. The trendlines in **c** and **d** represent the best fit, with corresponding power functions and R squared.

of our results are multifold. First, we confirm that intense trawling (SAR > 1 yr^{-1}) effectively reduces surface sediment carbon content[3,6]. Second, weak trawling intensity (SAR < 1 yr^{-1}) may increase or decrease local carbon storage due to an interplay of involved processes[4,5]. In addition, we found that carbon in muddy sediments is more susceptible to trawling impacts than in sand, and benthic fauna plays a critical role in OC storage and turnover.

A key uncertainty involved in the debates is related to the OC remineralization rate (k) in sediments, which may affect the estimate by over one order of magnitude[5,6]. In our simulations, k ranges generally between 10^{-3} and 3 yr^{-1} in surface sediments (Supplementary Fig. 9) and decreases downwards with depth similar to the pattern reported by ref. 5 The decrease is more pronounced in weakly trawled or untrawled areas (SAR < 1 yr^{-1}) than in heavily trawled areas (SAR > 5 yr^{-1}). Unfortunately, we do not have measurements of k for a direct comparison with simulation results. Instead, measured C/N ratio and chlorophyll a/OC ratio were used as a proxy for lability of OC and compared with simulation results in our previous studies[27,29]. In addition, we have simulated sediment oxygen consumption rates, which also serve as an indicator for k[43]. Nevertheless, direct support for k values in surface sediments is needed to better constrain the estimation uncertainty. According to our results, the spatially averaged, long-term reduction of OC storage capacity in the North Sea is ~1 MgC km^{-2} yr^{-1} (Fig. 3), equivalent to emission of 3.67 MgCO$_2$ km^{-2} yr^{-1} if all reduced OC is turned into CO$_2$. This reduction is less than 0.5% of the gross annual primary production (~230 MgC km^{-2} yr^{-1}) in the North Sea[44].

To compare with the existing global estimates, the result of the North Sea is upscaled by two approaches: (1) a linear scaling based on the ratio of the global bottom-trawling effort[23] to the regional value and (2) linear scaling using (1) but distinguished between sand and muddy sediments[45,46]. The first approach produces a result of 0.01 PgC yr^{-1} (equivalent to emission of 0.037 Pg CO$_2$ yr^{-1} if all reduced OC is turned into CO$_2$) for a global reduction of OC stock in shelf sea sediments, while the second approach yields a value of 0.008 PgC yr^{-1} (equivalent to emission of 0.03 PgCO$_2$ yr^{-1}). Our estimates are less than 10% of the original global estimate (0.58 PgCO$_2$ yr^{-1}) of ref. 3 but comparable to their later estimate (0.043 PgCO$_2$ yr^{-1}) using a lower k value[6]. The large discrepancy between our estimate and that of ref. 3 is not surprising since the redeposition of resuspended OC and the impact of trawling on benthic fauna, which partly offset the loss of OC, are not considered by ref. 3 Further, freshly deposited OC may undergo various cycles of resuspension–transport–deposition before its burial. The OC content in surface sediments may have large seasonal variability. This is seen in our simulation results (No trawling scenario) showing remarkably increased deposition of labile OC originated from primary production in late spring and summer when hydrodynamics is mild, while most of the labile OC in surface sediments is depleted in stormy winter (Supplementary Fig. 10). This result suggests that a large portion of OC, especially labile and semi-labile components, is remineralized naturally even without trawling (Fig. 3c). Another source of discrepancy originates from assessment of the impact of weak trawling intensity (SAR < 1 yr^{-1}). According to our estimate (Fig. 1a), most trawled areas in
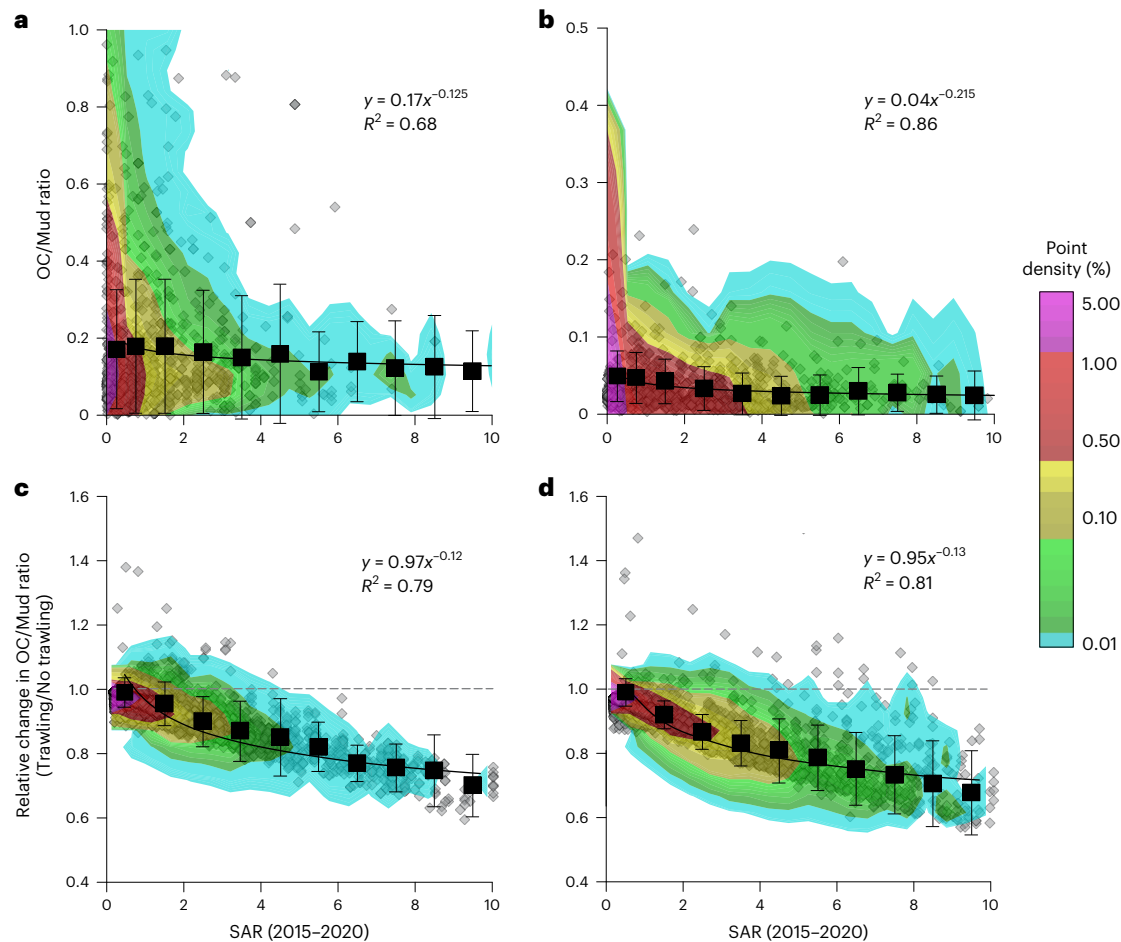
Fig. 6 | Difference in carbon storage and response to trawling impact between sand and muddy sediments in the North Sea. a, Distribution of surface sediment OC/mud measured in sand ($n = 1,031$) in relation to the multi-year averaged SAR. The means ± standard deviations are indicated by dots and error bars. **b**, Similar to **a** but for muddy sediments ($n = 1,349$). **c**, Relative change of OC/mud in sand between simulations with and without trawling for 50 years. **d**, Similar to **c** but for muddy sediments. The trendlines represent the best fit, with corresponding power functions and R squared.

global shelf seas have SAR < 1 yr⁻¹. In these areas, both gain and loss of OC could occur. Our simulations demonstrate that OC content is generally increased in untrawled and weakly trawled areas that are located near intensely trawled areas due to deposition of resuspended OC from those areas (Fig. 4). Given that areas of weak trawling (SAR < 1 yr⁻¹) take up the majority of all trawled grounds at a global scale, it is crucial to disentangle the feedback among involved processes in these areas for a reliable estimate of trawling-induced net OC change.

Our results in Fig. 5 suggest that the change of OC/mud occurs most rapidly in the first few years when trawling is implemented. Afterwards, the rate of change slows, and the difference in OC/mud between the results of 10 and 50 years of continuous trawling is only a few percentage points. This indicates a fast system response of OC/mud to trawling in the initial period towards a quasi-steady state at longer term. This evolution trend is in line with ref. 47, which suggests a stabilization of trawling-induced CO_2 emissions after 7–9 years of persistent trawling. Drawing on this, ref. 47 proposed that maximum benefits in reducing bottom fisheries' contribution to rising atmospheric CO_2 would appear 7–9 years after implementation of management policies. However, restoration of full capacity of carbon storage in surface sediments may require much longer, particularly in areas with low sedimentation rates. Taking the North Sea, for example, sedimentation rates are less than 1 mm yr⁻¹ in more than 75% of the seabed, and enhanced values (up to 6 mm yr⁻¹) appear only in spatially confined mud depocentres[18]. Our model projection shows that the restoration of carbon stock in surface sediments would

require several decades with a complete cessation of bottom trawling (Supplementary Fig. 6).

Online content

Any methods, additional references, Nature Portfolio reporting summaries, source data, extended data, supplementary information, acknowledgements, peer review information; details of author contributions and competing interests; and statements of data and code availability are available at https://doi.org/10.1038/s41561-024-01581-4.

References

1. Oberle, F. K. J., Storlazzi, C. D. & Hanebuth, T. J. J. What a drag: quantifying the global impact of chronic bottom trawling on continental shelf sediment. *J. Mar. Syst.* **159**, 109–119 (2016).
2. Halpern, B. S. et al. A global map of human impact on marine ecosystems. *Science* **319**, 948–953 (2008).
3. Sala, E. et al. Protecting the global ocean for biodiversity, food and climate. *Nature* **592**, 397–402 (2021).
4. Epstein, G., Middelburg, J. J., Hawkins, J. P., Norris, C. R. & Roberts, C. M. The impact of mobile demersal fishing on carbon storage in seabed sediments. *Glob. Change Biol.* **28**, 2875–2894 (2022).
5. Hiddink, J. G. et al. Quantifying the carbon benefits of ending bottom trawling. *Nature* https://doi.org/10.1038/s41586-023-06014-7 (2023)

6. Atwood, T. B. et al. Reply to: Quantifying the carbon benefits of ending bottom trawling. *Nature* https://doi.org/10.1038/s41586-023-06015-6 (2023)

7. Hiddink, J. G. et al. Global analysis of depletion and recovery of seabed biota after bottom trawling disturbance. *Proc. Natl Acad. Sci. USA* **114**, 8301–8306 (2017).

8. Amoroso, R. O. et al. Bottom trawl fishing footprints on the world's continental shelves. *Proc. Natl Acad. Sci. USA* **115**, E10275–E10282 (2018).

9. Tiano, J. C. et al. Trawling effects on biogeochemical processes are mediated by fauna in high-energy biogenic-reef-inhabited coastal sediments. *Biogeosciences* **19**, 2583–2598 (2022).

10. De Borger, E., Tiano, J., Braeckman, U., Rijnsdorp, A. D. & Soetaert, K. Impact of bottom trawling on sediment biogeochemistry: a modelling approach. *Biogeosciences* **18**, 2539–2557 (2021).

11. Lee, C., Wakeham, S. & Arnosti, C. Particulate organic matter in the sea: the composition conundrum. *Ambio* **33**, 565–575 (2004).

12. Ho, Q. N., Fettweis, M., Spencer, K. L. & Lee, B. J. Flocculation with heterogeneous composition in water environments: a review. *Water Res.* **213**, 118147 (2022).

13. Hartnett, H., Keil, R., Hedges, J. & Devol, A. H. Influence of oxygen exposure time on organic carbon preservation in continental margin sediments. *Nature* **391**, 572–575 (1998).

14. Xu, S., Liu, B., Arndt, S., Kasten, S. & Wu, Z. Assessing global-scale organic matter reactivity patterns in marine sediments using a lognormal reactive continuum model. *Biogeosciences* **20**, 2251–2263 (2023).

15. Keil, R. G. & Hedges, J. I. Sorption of organic matter to mineral surfaces and the preservation of organic matter in coastal marine sediments. *Chem. Geol.* **107**, 385–388 (1993).

16. Blair, N. E. & Aller, R. C. The fate of terrestrial organic carbon in the marine environment. *Annu. Rev. Mar. Sci.* **4**, 401–423 (2012).

17. Bianchi, T. S. et al. Anthropogenic impacts on mud and organic carbon cycling. *Nat. Geosci.* **17**, 287–297 (2024).

18. Diesing, M., Thorsnes, T. & Bjarnadóttir, L. R. Organic carbon densities and accumulation rates in surface sediments of the North Sea and Skagerrak. *Biogeosciences* **18**, 2139–2160 (2021).

19. Wilson, R. J., Speirs, D. C., Sabatino, A. & Heath, M. R. A synthetic map of the north-west European shelf sedimentary environment for applications in marine science. *Earth Syst. Sci. Data* **10**, 109–130 (2018).

20. Atwood, T. B., Witt, A., Mayorga, J., Hammill, E. & Sala, E. Global patterns in marine sediment carbon stocks. *Front. Mar. Sci.* **7**, 165 (2020).

21. Lee, T. R., Wood, W. T. & Phrampus, B. J. A machine learning (kNN) approach to predicting global seafloor total organic carbon. *Glob. Biogeochem. Cycles* **33**, 37–46 (2019).

22. Eigaard, O. R. et al. The footprint of bottom trawling in European waters: distribution, intensity, and seabed integrity. *ICES J. Mar. Sci.* **74**, 847–865 (2017).

23. Kroodsma, D. A. et al. Tracking the global footprint of fisheries. *Science* **359**, 904–908 (2018).

24. Pitcher, C. R. et al. Trawl impacts on the relative status of biotic communities of seabed sedimentary habitats in 24 regions worldwide. *Proc. Natl Acad. Sci. USA* **119**, e2109449119 (2022).

25. Thurstan, R., Brockington, S. & Roberts, C. The effects of 118 years of industrial fishing on UK bottom trawl fisheries. *Nat. Commun.* **1**, 15 (2010).

26. Middelburg, J. J. Reviews and syntheses: to the bottom of carbon processing at the seafloor. *Biogeosciences* **15**, 413–427 (2018).

27. Zhang, W. & Wirtz, K. Mutual dependence between sedimentary organic carbon and infaunal macrobenthos resolved by mechanistic modeling. *J. Geophys. Res. Biogeosci.* **122**, 2509–2526 (2017).

28. Rooze, J. et al. Bottom-trawling signals lost in sediment: a combined biogeochemical and modeling approach to early diagenesis in a perturbed coastal area of the southern Baltic Sea. *Sci. Total Environ.* **906**, 167551 (2024).

29. Zhang, W. et al. The budget of macrobenthic reworked organic carbon—a modelling case study of the North Sea. *J. Geophys. Res. Biogeosci.* **124**, 1446–1471 (2019).

30. Zonneveld, K. A. F. et al. Selective preservation of organic matter in marine environments; processes and impact on the sedimentary record. *Biogeosciences* **7**, 483–511 (2010).

31. Keil, R. Anthropogenic forcing of carbonate and organic carbon preservation in marine sediments. *Annu. Rev. Mar. Sci.* **9**, 151–172 (2017).

32. Freitas, F. S. et al. New insights into large-scale trends of apparent organic matter reactivity in marine sediments and patterns of benthic carbon transformation. *Biogeosciences* **18**, 4651–4679 (2021).

33. van de Velde, S. et al. Anthropogenic disturbance keeps the coastal seafloor biogeochemistry in a transient state. *Sci. Rep.* **8**, 5582 (2018).

34. Dounas, C. et al. Large-scale impacts of bottom trawling on shelf primary productivity. *Cont. Shelf Res.* **27**, 2198–2210 (2007).

35. Martín, J., Puig, P., Palanques, A., Masqué, P. & García-Orellana, J. Effect of commercial trawling on the deep sedimentation in a Mediterranean submarine canyon. *Mar. Geol.* **252**, 150–155 (2008).

36. Paradis, S. et al. Spatial distribution of sedimentation-rate increases in Blanes Canyon caused by technification of bottom trawling fleet. *Prog. Oceanogr.* **169**, 241–252 (2018).

37. Kaiser, M. J. et al. Global analysis of response and recovery of benthic biota to fishing. *Mar. Ecol. Prog. Ser.* **311**, 1–14 (2006).

38. Sciberras, M. et al. Response of benthic fauna to experimental bottom fishing: a global meta-analysis. *Fish Fish.* **19**, 698–715 (2018).

39. Tillin, H. M., Hiddink, J. G., Jennings, S. & Kaiser, M. J. Chronic bottom trawling alters the functional composition of benthic invertebrate communities on a sea-basin scale. *Mar. Ecol. Prog. Ser.* **318**, 31–45 (2006).

40. Tiano, J. C. et al. Acute impacts of bottom trawl gears on benthic metabolism and nutrient cycling. *ICES J. Mar. Sci.* **76**, 1917–1930 (2019).

41. LaRowe, D. E. et al. The fate of organic carbon in marine sediments—new insights from recent data and analysis. *Earth Sci. Rev.* **204**, 103146 (2020).

42. Rijnsdorp, A. D. et al. Estimating sensitivity of seabed habitats to disturbance by bottom trawling based on the longevity of benthic fauna. *Ecol. Appl.* **28**, 1302–1312 (2018).

43. Zhang, W. et al. Quantifying importance of macrobenthos for benthic–pelagic coupling in a temperate coastal shelf sea. *J. Geophys. Res. Oceans* **126**, e2020JC016995 (2021).

44. Capuzzo, E. et al. A decline in primary production in the North Sea over 25 years, associated with reductions in zooplankton abundance and fish stock recruitment. *Glob. Change Biol.* **24**, e352–e364 (2018).

45. Jenkins, C. Building offshore soils databases. *Sea Technol.* **38**, 25–28 (1997).

46. Bostock, H. et al. Distribution of surficial sediments in the ocean around New Zealand/Aotearoa. Part B: continental shelf. *N. Z. J. Geol. Geophys.* **62**, 24–45 (2019).

47. Atwood, T. B. et al. Atmospheric CO_2 emissions and ocean acidification from bottom-trawling. *Front. Mar. Sci.* **10**, 1125137 (2024).

[1]Institute of Coastal Systems—Analysis and Modeling, Helmholtz-Zentrum Hereon, Geesthacht, Germany. [2]GEOMAR-Helmholtz Centre for Ocean Research Kiel, Kiel, Germany. [3]Institute of Carbon Cycles, Helmholtz-Zentrum Hereon, Geesthacht, Germany. [4]Alfred Wegener Institute Helmholtz Centre for Polar and Marine Research, Bremerhaven, Germany. [5]MARUM—Center for Marine Environmental Sciences, University of Bremen, Bremen, Germany. [6]Faculty of Geosciences, University of Bremen, Bremen, Germany. [7]BUND-Meeresschutzbüro, Bund für Umwelt und Naturschutz Deutschland e.V. (BUND), Bremen, Germany. [8]Hamburg Institute of International Economics (HWWI), Hamburg, Germany. [9]Helmut Schmidt University Hamburg, Hamburg, Germany. [10]Institute of Oceanography, Center for Earth System Research and Sustainability, University of Hamburg, Hamburg, Germany. ✉e-mail: wenyan.zhang@hereon.de

Methods

Sediment data

Surface sediment OC and mud content in the North Sea based on measurement of sediment samples (n = 2,380; Supplementary Fig. 4) from various German and European surveys conducted since 1980s have been compiled in refs. 48–50 and were analysed in this study. In addition, field data from other literature and recently collected sediment samples in both frequently trawled and untrawled areas were included for assessment of model performance (Supplementary Table 2). Sediment and macrobenthos samples were collected from these stations by means of a multicorer (Oktopus Kiel). Vertical distributions of total organic carbon (TOC), TOC/total nitrogen ratio and macrobenthos biomass in the uppermost 20 cm sediments were measured[29]. In the southern North Sea stations, bioturbation rates were estimated mostly by evaluation of chlorophyll profiles[51]. Chlorophyll was extracted from freeze-dried sediment with 90% acetone and measured subsequently. The depth gradient of chlorophyll was then evaluated with Fick's first law of diffusion to derive the bioturbation rate. In the Skagerrak stations, bioturbation rates were estimated by simulating the depth distribution of ^{210}Pb (ref. 52) using a steady-state transport–reaction model[27].

Bottom-trawling data

Annual aggregated spatial data on bottom trawling in the North Sea including gear-type information[53] were combined with daily fishing effort data[23] to generate a daily time series of fishing effort on a 0.05° × 0.05° grid. The multi-year (2015–2020) averaged data were used for analysis of the linkage between trawling density and OC/mud, while the daily time series served as input for numerical modelling.

A daily time series of bottom-trawling impact was generated from the dataset of ref. 23, which contains daily vessel locations and fishing effort as well as estimates of vessel power, length and class but does not distinguish between specific gear types. For each vessel designated as a 'trawler', we assigned a gear type according to the dominant 'métier', following the definition in ref. 54, and by co-locating the vessel positions to the International Council for Exploration of the Sea (ICES) métiers, as explained in ref. 55. A métier groups fishing trips by gear type and target species. In the North Sea, otter and beam trawlers are dominant and account for more than 90% of total annual fishing effort[53]. The ropes of demersal seines are expected to have no subsurface (>2 cm) impacts. Dredges are expected to have a high impact per surface area contacted[56], but they are confined within a small area[53].

For each grid cell, the daily surface SAR (SAR_d) was calculated following the method by ref. 55. We estimated the daily SAR in three depth intervals within the seabed: 0–2 cm, 2–- cm and 5–10 cm. Muddy and sandy areas are distinguished when computing the SAR at different penetration depths. The depth to which the individual gear components penetrate in sandy and muddy sediment were determined using information given in ref. 54 (Supplementary Table 3). The mud fraction of the sediment was assigned according to the surface sediment map provided in ref. 50.

A comparison between the annual aggregated bottom-trawling effort from ICES, which is based on the Vessel Monitoring System[53] and logbook data, and daily fishing effort data, which are based on the self-reported Automatic Identification System (AIS)[23], shows a consistency for recent years (2015–2020; Supplementary Fig. 11). The annual aggregated trawling effort from the AIS-based data are lower than the ICES data in early years. Starting from 2018, both datasets yield comparable results within ±5% difference[55]. However, the AIS-based data substantially underestimate the bottom-trawling effort in early years[55]. This deficit impedes the use of the AIS-based data as input for numerical modelling for long-term (decadal) historical hindcast. To derive a consistent daily resolved long-term time series of trawling data before 2015 for numerical modelling, we averaged the daily SAR fields of 2015–2020 and scaled them with reported historical data. For the period 1985–2014, a historical reconstruction of annual aggregated

bottom-trawling effort has been compiled in ref. 57. Their outcomes suggest a stable distribution of fishing effort among countries, seasons and gear types for the 30 year period. Such stable distribution is also seen in the ICES 2015–2020 data[53] (see also Supplementary Figs. 12–14). On the basis of this stability, the spatial and daily distribution of fishing effort in the historical period 1950–2014 is assumed to follow the same spatial and seasonal pattern as in 2015–2020 but is scaled by the ratio of the annual aggregated trawling effort for the specific year to the average of the years 2015–2020. For the period 1950–1984, in which annual aggregated trawling data are missing, we employed three scaling methods to generate the spatio-temporal distribution of daily effort. Method 1 is based on the relationship between trawling effort and total annual landings. The time series of bottom-trawling effort for 1985–2020 shows a high correlation (r = 0.86) with the annual landing data of demersal and benthic fish (ICES[58]; Supplementary Fig. 15). On the basis of this correlation, we extrapolated the time series of annual aggregated bottom-trawling effort for 1950–1984 through a linear regression between the trawling and landing data. Method 2 is based on the relationship between the total trawling effort in the North Sea and the United Kingdom's portion. Among all North Sea countries, trawling data from the United Kingdom have the longest temporal coverage dating back to the 1910s[59]. The trawling effort of UK vessels shows an almost linear (r = 0.98) relationship with the total effort in the North Sea in 2003–2020. On the basis of this relationship, the total trawling effort for 1950–1984 was assumed to also scale linearly with the UK trawling effort. In Method 3, we considered an increase of technological efficiency, or 'creep factor,' which is used in fisheries science to adjust for the gradual increase in the effectiveness of fishing gear resulting from the successive introduction of technological improvement to fishing gear and vessels[60]. We adopted a technological creep factor of 2.4% yr^{-1} (ref. 60) in scaling the trawling effort with the total annual landings. The resulting time series from the three scaling methods (Supplementary Fig. 15) help to evaluate the sensitivity of sedimentary OC stock to long-term temporal variability of trawling effort.

Synthesis of sediment and bottom-trawling data

Since sediment data (mud and OC content) and bottom-trawling intensity represented by multi-year (2015–2020) averaged SAR are derived from independent sources, we synthesized these data by pairing the point data of sediment mud and OC content with the nearest SAR value calculated at a 0.05° × 0.05° grid. In the synthesized dataset, we aggregated the data into intervals defined by ΔSAR between SAR = 0 and 10 yr^{-1} and calculated the mean and standard deviation of OC/mud in each interval. We ensured that the number of points in each interval is within the same order of magnitude for statistical analysis (Fig. 1 and Supplementary Fig. 3). Data with SAR > 10 yr^{-1} are integrated into the interval 9 yr^{-1} ≤ SAR ≤ 10 yr^{-1} because of their small sample size (12 out of 2,380 points).

Multivariate analysis

We conducted a linear multivariate regression analysis using ordinary least squares on the North Sea point data, with OC as the dependent variable and SAR as the main independent variable. In addition to mud content (mud), we performed regressions using several covariates that could affect OC, including water depths (depth) from EMODnet[61]; bed shear stresses (tau), bottom phytoplankton concentrations (phy) and bottom water temperatures (temp) derived from the long-term (1950–2016) averages of simulation results (see 'Numerical modelling' below); and shortest distance to the coast (dist) from the AIS-based data[23].

The potential endogeneity of fishing effort poses a challenge in the regression analysis as sediment OC or mud content could potentially affect fishing activity, resulting in bidirectional causality. To address the endogeneity problem, we additionally employed an instrumental variables approach using a fuzzy regression discontinuity design. The results show a statistically significant negative impact of SAR

on OC, confirming the results of the ordinary least squares estimate (Supplementary Text 1).

Numerical modelling

We applied a three-dimensional physical–biogeochemical model to simulate the impact of bottom trawling on macrobenthos and OC cycling in surface sediments. The model consists of three major components, with HAMSOM (Hamburg Shelf Ocean Model[62]) for hydrodynamics, ECOSMO (EcoSystem Model[63]) for biogeochemistry and TOCMAIM (Total Organic Carbon–Macrobenthos Interaction Model[43]) for benthic fauna and early diagenesis of OC. The OC is divided into three pools depending on its degradability: labile (of high nutritional quality for macrobenthos with first-order oxic remineralization rate $k = 20$ yr^{-1}), semi-labile (of intermediate nutritional quality with $k = 2$ yr^{-1}), and refractory (of low nutritional quality with $k = 0.01$ yr^{-1}) (ref. 43). With a Neumann boundary condition of OC fluxes at the sediment–water interface calculated by the pelagic model component (ECOSMO), sedimentary OC content is solved by a mass balance equation in TOCMAIM, including the impacts of deposition/erosion, oxygen-dependent first-order degradation, macrobenthic uptake, respiration and bioturbation[43]. Temporal change of macrobenthic biomass is calculated on the basis of food availability in the form of OC, temperature, oxygen, and mortality caused by predation and bottom trawling. Bioturbation scales with macrobenthic biomass and is inversely related to local OC resource[27]. The fractions of labile, semi-labile and refractory OC in the freshly deposited phytoplanktonic detritus are determined as 0.33, 0.45 and 0.22, respectively, on the basis of model calibration with station data[29]. Suspended particulate OC is assumed to have the same settling velocity as silt (0.1 mm s^{-1}) (ref. 55). Oxygen penetration depth is jointly determined by physical (sediment permeability, porosity, bedform and bottom current velocity) and biogeochemical (carbon remineralization) parameters[43]. A basic assumption in the sediment model (TOCMAIM) is that OC remineralization is controlled by oxygen, with a larger rate in the oxic condition than in the anoxic condition[29]. The first-order remineralization rate k for each OC pool is defined as the rate in the oxic condition. With the oxygen penetration depth σ calculated in the sediment model, a depth dependency of k for each OC pool in sediment (that is, $k(z) = k(\sigma)e^{-0.3z}$, where z refers to the depth below σ) is introduced to mimic the impact of oxygen on remineralization of OC. The sediment OC content is updated at a daily scale.

The model has been applied to the North Sea to investigate the spatio-temporal variability of macrobenthic biomass[27,29], sediment OC storage[29] and benthic oxygen consumption[43]. Details of mathematical descriptions, sensitivity analysis of model parameters and application to station data are provided in ref. 27. Model coupling between benthic and pelagic components as well as its application to the North Sea are introduced in refs. 29,43.

The long-term hindcast simulation encompasses the period 1950–2016 in two repetitive loops. The first loop is used as a spin-up to reach a state of quasi-equilibrium of OC distribution in surface sediments. The map of surface sediment OC content (Supplementary Fig. 1b) is used as the initial condition assuming that all OC is refractory so that associated benthic variables, including macrobenthic biomass, bioturbation and oxygen consumption rate, are initiated from low level to avoid unexpected bias, errors or spurious fluctuations in the computation. Input of labile and semi-labile OC to sediment is provided by the pelagic model component, which simulates the primary production and associated OC fluxes during the period 1950–2016[29]. Because macrobenthic biomass is dependent on both quality and quantity of sedimentary OC, simulation of the first three decades is featured by an increase of biomass due to gradual accumulation of labile and semi-labile OC in sediments. Afterwards, the simulated macrobenthic biomass and OC fluxes across the sediment–water interface approach a relatively stable level[29]. After completion of the first loop of simulation (1950–2016), the model continues simulation with the forcing starting from 1950 again. In this loop, different scenarios of trawling impacts (Supplementary Table 1) are implemented. Simulation results from the second loop were used for evaluation of the benthic OC fluxes with and without trawling.

In addition, to estimate the restoration potential of sedimentary OC after cessation of bottom trawling, the simulation in the scenario representing the highest trawling impact on sedimentary OC stock continued in a third loop with cessation of trawling.

Numerical implementation of trawling impacts

The impact of bottom trawling on OC storage in sediments is implemented through enhanced OC resuspension and subsequent transport, physical mixing in the penetrated sediments and enhanced mortality of macrobenthos, which subsequently affect macrobenthic uptake of OC, respiration and bioturbation intensity.

To estimate the resuspension rate of each trawler in the daily resolved data, we follow ref. 64, which demonstrated that sediment entrained behind towed fishing gear is directly related to the hydrodynamic drag of the fishing gear components and to the seafloor sediment type. A detailed description of the calculation is provided in ref. 55. The calculated average resuspension per area contacted is 2.1 kg m^{-2} with a standard deviation of 1.6 kg m^{-2}, which is well within the range of reported values (0.5–6.0 kg m^{-2}). The resuspension is divided among mud and sand according to their fraction in the seabed (Supplementary Fig. 1a). Accordingly, OC in surface sediment is also resuspended according to its weight proportion in the sediment[65]. At each model time step, the trawling-induced resuspension flux is added to the hydrodynamic resuspension flux. Resuspended OC of each pool that is exposed to oxic bottom water is remineralized with the corresponding first-order remineralization rate k.

For implementation of trawling impact on benthic fauna, three impact levels in mortality—low (10th percentile, corresponding to a depletion rate of 0.11 for SAR = 1 yr^{-1}), medium (50th percentile/depletion rate of 0.2) and high (90th percentile/depletion rate of 0.3)—were included according to field assessments[7,66]. Trawling-induced daily mortality M (day^{-1}) is then calculated by:

$$M = \text{SAR} \times I,$$

where $I = 0.11/0.2/0.3$ refers to the low/medium/high mortality ratio, respectively; M is divided into three depth layers (0–2 cm, 2–5 cm and 5–10 cm) according to the corresponding SAR values in these zones (Supplementary Table 3).

In addition, the impact of physical mixing was implemented as a mixing coefficient[10] scaled by SAR in the impacted sediment layers. Due to lack of data support for determining the physical mixing coefficient in field, we adopted two constant values, 2.40 and 0.24 cm^2 day^{-1}, representing high and low mixing efficiency[55], respectively, in the model experiments to estimate the associated uncertainty in the result. The mixing coefficient is multiplied by the daily SAR to calculate daily matter fluxes (OC and oxygen).

The three generated time series of trawling, combined with the different impact levels of trawling-induced faunal mortality and physical mixing, produce in total 18 different scenarios (Supplementary Table 1). These scenarios were compared with a non-trawling scenario (No trawling).

Validation of numerical modelling

Our simulation results have been confirmed by field data of OC, oxygen consumption rate and macrobenthic biomass in seafloor surface sediments of the southern North Sea[29,43]. In this study, the model domain was extended to the entire North Sea, and additional field data from the northern part (Supplementary Table 2) were compiled. The measured

OC data, macrobenthos biomass and estimated bioturbation rates at these field stations were used to assess the simulation results.

A comparison between the simulated mean values of the 18 experiments with trawling impact and field data suggests a generally satisfactory model performance in capturing spatial distribution of OC content (Fig. 5b), macrobenthic biomass and bioturbation rates (Supplementary Fig. 16). The correlation coefficients (Pearson's *r*) between the measured and simulated values for macrobenthic biomass (in ash-free dry weight) and bioturbation rate are 0.91 and 0.71, respectively. The root mean square error for biomass is 2.23 g m^{-2}, equivalent to 40% of the spatially averaged biomass in the North Sea. The simulated spatial distribution of biomass along latitude (Supplementary Fig. 16b) also shows consistency with data from two large-scale surveys[67]. The normalized root mean square error for bioturbation rate is 0.176. It is worth noting that the estimated bioturbation rates from fitting tracer profiles (chlorophyll and ^{210}Pb) vary over one order of magnitude within the samples from each field station. This may be due partly to difference in the estimations using different tracers and partly to small-scale heterogeneity of bioturbation driven by variations in food supply[27] and metabolism rate of benthic fauna[64,68] as well as sediment composition and community structure[25,69–71]. Although the model grid (0.03° × 0.03°) is too coarse to resolve such heterogeneity at small spatial scales, the mean bioturbation rate from the samples at each station was reasonably captured by the simulations.

Assessing uncertainty in the relationship between OC/mud and SAR

Trawling intensity represented by SAR may differ among individual years; therefore, we calculated the multi-year averaged SAR to (1) avoid a single-year bias and (2) obtain a longer-term, accumulative impact that can be reflected in sediment signals. Existing studies show that bottom-trawling locations appear to be consistent from year to year in most regions as illustrated by global data from refs. 8,72 and by regional data from the North Sea dating back to the 1980s. Although the locations of trawling remain stable, year-to-year variations as well as a longer-term change of trawling intensity do exist (Supplementary Fig. 15). The impacts are elevated in years with higher trawling intensity according to our simulation results (Supplementary Figs. 5 and 6). However, because of a rapid system response of OC/mud in surface sediments to trawling in the initial period towards a quasi-steady state at longer timescales, annual variations of trawling intensity cause fluctuations but not systematic deviations from the quasi-steady state (Fig. 5c,d). Further, recovery of OC/mud in undisturbed sediment would require much longer time than the time scale of trawling, particularly on a seabed with a low sedimentation rate. Hence, we are confident in stating that despite uncertainties in the calculation of SAR, the relationship between OC/mud and multi-year (2015–2020) averaged SAR is robust.

Data availability
Datasets for this research are available via Zenodo (https://doi.org/10.5281/zenodo.8297751) (ref. 73). Previously published datasets used in this study are cited in Methods, with details listed in Supplementary Table 4.

Code availability
The source code of ECOSMO can be accessed via Zenodo at https://zenodo.org/records/6387608 (ref. 74). HAMSOM is available at https://csdms.colorado.edu/wiki/Model:HAMSOM. The source code of TOCMAIM with a coupling interface to 3-D hydrodynamic biogeochemical models is stored in Mendeley Data with open access at https://doi.org/10.17632/2vvny3xd85.2. The compiled North Sea dataset and code (R) for multivariate analysis is available via Zenodo at https://doi.org/10.5281/zenodo.13322571 (ref. 75).

References
48. Bockelmann, F. D. *Mud Content of North Sea Surface Sediments* (WDC Climate, 2017); https://doi.org/10.1594/WDCC/coastMap_Substrate_Mud
49. Bockelmann, F. D. *Total Organic Carbon Content of North Sea Surface Sediments* World Data Center for Climate (WDC Climate, 2017); https://doi.org/10.1594/WDCC/coastMap_Substrate_TOC
50. Bockelmann, F. D., Puls, W., Kleeberg, U., Müller, D. & Emeis, K. C. Mapping mud content and median grain-size of North Sea sediments—a geostatistical approach. *Mar. Geol.* **397**, 60–71 (2018).
51. Neumann, A. et al. Macrofauna as a major driver of bentho–pelagic exchange in the southern North Sea. *Limnol. Oceanogr.* **66**, 2203–2217 (2021).
52. Spiegel, T. et al. Modelling mass accumulation rates and ^{210}Pb rain rates in the Skagerrak: lateral sediment transport dominates the sediment input. *Front. Mar. Sci.* **11**, 1331102 (2024).
53. *OSPAR Request 2018 for Spatial Data Layers of Fishing Intensity/Pressure* (ICES, 2019); https://doi.org/10.17895/ices.data.4686
54. Eigaard, O. R. et al. Estimating seabed pressure from demersal trawls, seines, and dredges based on gear design and dimensions. *ICES J. Mar. Sci.* **73**, i27–i43 (2016).
55. Porz, L. et al. Quantification and mitigation of bottom-trawling impacts on sedimentary organic carbon stocks in the North Sea. *Biogeosciences* **21**, 2547–2570 (2024).
56. O'Neill, F. G., Robertson, M., Summerbell, K., Breen, M. & Robinson, L. A. The mobilisation of sediment and benthic infauna by scallop dredges. *Mar. Environ. Res.* **90**, 104–112 (2013).
57. Couce, E., Schratzberger, M. & Engelhard, G. H. Reconstructing three decades of total international trawling effort in the North Sea. *Earth Syst. Sci. Data* **12**, 373–386 (2020).
58. *Greater North Sea Ecoregion Fisheries Overview—Data Output File* (ICES, 2021); https://doi.org/10.17895/ices.data.9158
59. Engelhard, G. H. *North Sea Historical Effort by Rectangle by Month: 1913–1980* Version 1 (Cefas, 2016); https://doi.org/10.14466/CefasDataHub.24
60. Palomares, M. L. D. & Pauly, D. On the creeping increase of vessels' fishing power. *Ecol. Soc.* **24**, 31 (2019).
61. EMODnet Digital Bathymetry (DTM 2020) (EMODnet, 2020); https://doi.org/10.12770/bb6a87dd-e579-4036-abe1-e649cea9881a
62. Schrum, C. Thermohaline stratification and instabilities at tidal mixing fronts—results of an eddy resolving model for the German Bight. *Cont. Shelf Res.* **17**, 689–716 (1997).
63. Daewel, U. & Schrum, C. Simulating long-term dynamics of the coupled North Sea and Baltic Sea ecosystem with ECOSMO II: model description and validation. *J. Mar. Syst.* **119–120**, 30–49 (2013).
64. O'Neill, F. G. & Ivanović, A. The physical impact of towed demersal fishing gears on soft sediments. *ICES J. Mar. Sci.* **73**, i5–i14 (2016).
65. O'Neill, F. G. & Noack, T. The geometry and dynamics of Danish anchor seine ropes on the seabed. *ICES J. Mar. Sci.* **78**, 125–133 (2021).
66. Bergman, M. J. N. & Van Santbrink, J. W. Mortality in megafaunal benthic populations caused by trawl fisheries on the Dutch continental shelf in the North Sea in 1994. *ICES J. Mar. Sci.* **57**, 1321–1331 (2000).
67. *Structure and Dynamics of the North Sea Benthos* (ICES, 2007); https://doi.org/10.17895/ices.pub.5451
68. O'Neill, F. G. & Summerbell, K. The hydrodynamic drag and the mobilisation of sediment into the water column of towed fishing gear components. *J. Mar. Syst.* **164**, 76–84 (2016).

69. Teal, L. R., Bulling, M. T., Parker, E. R. & Solan, M. Global patterns of bioturbation intensity and mixed depth of marine soft sediments. *Aquat. Biol.* **2**, 207–218 (2008).

70. Solan, M. et al. Worldwide measurements of bioturbation intensity, ventilation rate, and the mixing depth of marine sediments. *Sci. Data* **6**, 58 (2019).

71. Morys, C., Forster, F. & Graf, G. Variability of bioturbation in various sediment types and on different spatial scales in the southwestern Baltic Sea. *Mar. Ecol. Prog. Ser.* **557**, 31–49 (2016).

72. Watson, R. A. A database of global marine commercial, small-scale, illegal and unreported fisheries catch 1950–2014. *Sci. Data* **4**, 170039 (2017).

73. Zhang, W. Field and model data for bottom trawling impacts in the North Sea. *Zenodo* https://doi.org/10.5281/zenodo.8297751 (2023).

74. Lisaeter, K. A. et al. HYCOM-ECOSMOII(CHL) a marine biogeochemical model for the North Atlantic and the Arctic model code and configuration. *Zenodo* https://zenodo.org/records/6387608 (2021).

75. Zhang, W. Data and code for analysis of bottom trawling impact on sedimentary organic carbon in the North Sea. *Zenodo* https://doi.org/10.5281/zenodo.13322571 (2024).

Author contributions

W.Z. designed the study. W.Z., L.P., R.Y., A.N. and T.S. compiled the data and conducted data analysis with inputs from F.-D.B., K.W., B.T., M.H., S.K., N.Z., H.T.M.H.-H. and J.K. L.B. performed the multivariate analysis. U.D. and C. S. provided the HAMSOM and ECOSMO models. W.Z. led the writing of the paper to which all co-authors contributed with comments and inputs.

Competing interests

The authors declare no competing interests.

Additional information

Extended data is available for this paper at https://doi.org/10.1038/s41561-024-01581-4.

Supplementary information The online version contains supplementary material available at https://doi.org/10.1038/s41561-024-01581-4.

Correspondence and requests for materials should be addressed to Wenyan Zhang.

Peer review information *Nature Geoscience* thanks Sarah Paradis, Craig Smeaton and the other, anonymous, reviewer(s) for their contribution to the peer review of this work. Primary Handling Editor: James Super, in collaboration with the *Nature Geoscience* team.

Reprints and permissions information is available at www.nature.com/reprints.

Extended Data Table 1 | Results of the multivariate linear regression on OC using OLS

Variable (unit)	Regression Results					
	(1)	(2)	(3)	(4)	(5)	(6)
SAR	0.059***	-0.021***	-0.013**	-0.017***	-0.015**	-0.016**
	(0.006)	(0.005)	(0.005)	(0.005)	(0.005)	(0.005)
mud (%)		0.014***	0.009***	0.010***	0.009***	0.009***
		(0.0004)	(0.0004)	(0.0004)	(0.0005)	(0.0005)
depth (m)			0.003***	0.003***	0.003***	0.003***
			(0.0001)	(0.0001)	(0.0002)	(0.0002)
dist (km)				-0.002***	-0.002***	-0.002***
				(0.0001)	(0.0002)	(0.0002)
temp (°C)					-0.019**	-0.023**
					(0.007)	(0.008)
tau (Pa)						-0.204
						(0.300)
phy (mg/m³)						0.0005
						(0.0005)
Constant	0.408***	0.237***	0.099***	0.252***	0.446***	0.467***
	(0.017)	(0.011)	(0.014)	(0.021)	(0.082)	(0.087)
Observations	2,380	2,380	2,380	2,380	2,175	2,175
Adjusted R^2	0.040	0.510	0.587	0.627	0.629	0.629
F Statistic	99.1***	1,236.9***	1,127.0***	1,001.1***	737.5***	526.7***

Robust standard errors are in parentheses. The p-values are based on two-sided tests. Number of observations is reduced for regressions (5) and (6) because some measurement locations are not covered by the domain of the numerical model used for temp, tau, and phy. No adjustments were made for multiple comparisons. ***$p < 0.001$, **$p < 0.01$, *$p < 0.05$.

Extended Data Table 2 | Results of the multivariate linear regression using OLS for subsamples of SAR

	Dependent variable: TOC	
	SAR < 1	SAR ≥ 1
SAR	0.011	-0.020**
	(0.037)	(0.008)
mud	0.019***	0.007***
	(0.001)	(0.001)
depth	0.001*	0.003***
	(0.0004)	(0.0004)
dist	-0.001***	-0.002***
	(0.0002)	(0.0003)
temp	-0.049***	-0.013
	(0.013)	(0.014)
tau	0.257	-0.125
	(0.428)	(0.465)
phy	0.001	-0.001
	(0.001)	(0.001)
Constant	0.600***	0.492***
	(0.130)	(0.139)
Observations	1,015	1,160
R^2	0.705	0.573
Adjusted R^2	0.703	0.570
Residual Std. Error	0.331 (df = 1007)	0.365 (df = 1152)
F Statistic	344.395*** (df = 7; 1007)	220.897*** (df = 7; 1152)

Robust standard errors are in parentheses. Number of observations are reduced for regressions (5) and (6) because some measurement locations are not covered by the domain of the numerical model used for *temp*, *tau* and *phy*. The p-values are based on two-sided tests. No adjustments were made for multiple comparisons. *** p<0.001, ** p<0.01, * p<0.05.

Extended Data Table 3 | Result of the Welch Two Sample t-test to compare the OC/mud between sand and muddy sediment types based on the North Sea point data

Habitat type	Sand	Muddy sediments
Mean	0.15083	0.02867
SD	0.1651	0.0254
Sample size	1031	1349
t	26.7733	
df	2378	
Standard error of difference	0.005	
P (one-tailed)	2.099E-19	
P (two-tailed)	4.199E-19	